Nitrous oxide activation by a cobalt(II) complex for aldehyde oxidation under mild conditions

Teresa Corona and Anna Company*

Grup de Química Bioinspirada, Supramolecular i Catàlisi (QBIS-CAT), Institut de Química Computacional i Catàlisi (IQCC), Departament de Química, Universitat de Girona, Campus Montilivi, 17071 Girona (Catalonia - Spain). Phone: +34 972 41 98 42. Fax: +34 972 41 81 50. E-mail: anna.company@udg.edu

Contents

1. Materials and methods

1.1. Instrumentation

Reagents and solvents used were commercially available and purchased from Panreac, Scharlau and Aldrich. Preparation and handling of air-sensitive materials were carried out in a N_2 drybox (MBraun ULK 1000) with O_2 and H_2O concentrations < 1 ppm. Commercially available superdry N_2O ($H_2O \leq$ 8ppm/v) from Abelló-Linde and O_2 >99.5% pure from Praxair were purchased and used as received. H_2L ligand was prepared following procedures described in the literature [T. Corona, F. F. Pfaff, F. Acuña-Parés, A. Draksharapu, C. J. Whiteoak, V. Martin-Diaconescu, J. Lloret-Fillol, W. R. Browne, K. Ray and A. Company, *Chem. Eur. J.,* **2015**, *21*, 15029-15038].

Elemental analyses of C, H and N were performed with a Perkin Elmer EA2400 series II elemental analyzer. Mass spectra were performed by electrospray ionization in a high-resolution mass spectrometer Bruker micrOTOF QII (Q-TOF) with a quadrupole analyzer with positive and negative ionization modes. ^{1}H-NMR, ^{13}C-NMR, COSY and HSQC spectra were performed in a Bruker Ultrashield Avance III400 and Ultrashield DPX300 spectrometers. UV-Vis spectra were performed by a diode array spectrophotometer Agilent Cary 60 and low temperature control was maintained with a cryostat from Unisoku Scientific Instruments. X-Ray analyses were carried out on a Bruker AXS SMART APEX CCD diffractometer using Mo Kα monochromatic radiation (λ = 0.71073 Å). Cyclic voltammetries were performed using a potentiostat from CHInstruments with a three electrode cell. The working electrode is a glassy carbon disk from BAS (0.07 cm^2), the reference electrode is a Ag^0/Ag^+ and the auxiliary electrode is platinum wire. All voltammetries have been carried out with $n Bu_4NPF_6$ (TBAP) as supporting electrolyte (0.1 M ionic strength) under N_2. GC analyses were carried out on an Agilent 7820A gas chromatograph (HP5 column, 30m) with a flame ionization detector. GC-MS spectral analyses were performed on an Agilent 7890A gas chromatograph interfaced with an Agilent 5975c mass spectrometer with Triple-axis detector. N_2 identification was carried out with an Agilent 7820A GC system equipped with three columns: washed molecular sieves 5Å, 2 m × 1/8 inch outside diameter (OD), Mesh 60/80 SS and Porapak Q, 4 m × 1/8 inch OD, Mesh 80/100 SS, and a thermal conductivity detector. Perpendicular mode X-band electron paramangetic responance (EPR) spectra were collected using a Bruker ESP 300E spectrometer. All EPR spectra were recorded at 77K with the following experimental parameters: frequency, 9.39 GHz; power 0.3 mW; modulation amplitude, 32 G; time constant, 20.48 s; conversion time, 80 s.

1.2. Synthesis of cobalt complexes

Synthesis of the [Co^{II}(CF$_3$SO$_3$)$_2$(CH$_3$CN)$_2$]. In a 100 mL Schlenk flask, CoCl$_2$ (4.9 g, 0.038 mmol) was dissolved with 30 mL of dry CH$_3$CN. Then, about Me$_3$SiOTf (14.5 mL, 0.080 mmol) was added to the solution under a N$_2$ atmosphere and allowed to stir at room temperature for 24 hours. A red colored solution appeared with a pale red precipitate. Then, the solvent was removed completely with a rotary evaporator. The resulting solid was dissolved again in CH$_3$CN (10 mL) and slow diethyl ether diffusion at room temperature over the resultant solution afforded a pink powder solid (12.7 g, 0.029 mmol, 76%). Anal. Calcd for $C_6H_6CoF_6N_2O_6S_2 \cdot 2H_2O$: C, 15.16; N, 5.90; H, 2.12 %. Found: C, 15.13; N, 5.65; H, 2.16 %.

Synthesis of [Co^{II}(L)]·KCF$_3$SO$_3$ (1·KCF$_3$SO$_3$). In the glove box, a solution of [Co(CH$_3$CN)$_2$(CF$_3$SO$_3$)$_2$] (16.7 mg, 0.038 mmol) in anhydrous CH$_3$CN (0.5 mL) was added dropwise to a vigorously stirred solution of H$_2$**L** (9.8 mg, 0.038 mmol) in anhydrous CH$_3$CN (0.5 mL). After a few seconds the solution turned orange. Addition of 2 equiv K[N(SiMe$_3$)$_2$] (15.2 mg, 0.076 mmol) caused a clear color change to dark red. After stirring for 3 hours, the solution was filtered through silica and concentrated. Slow diethyl ether diffusion over the resulting solution afforded, in a few days, dark red powder (co-crystallization with KCF$_3$SO$_3$) (11.0 mg, 0.022 mmol, 58 %). ESI-MS (m/z): 319.0590 [Co+L]$^+$, 342.0476 [**1**+Na]$^+$, 358.0238 [**1**+K]$^+$. CV (CH$_3$CN vs SCE) $E_{1/2} = 0.17$ V. $\mu_{eff} = 1.69\ \mu_B$ (Evans' method).

Synthesis of [Co^{III}(L)(acac)] (**2**). A solution of [Co(acac)$_3$] (24.8 mg, 0.060 mmol) in CH$_3$CN (0.5 mL) was added dropwise to a vigorously stirred solution of H$_2$**L** (15.8 mg, 0.060 mmol) in CH$_3$CN (0.5 mL). After a few seconds the solution turned dark green. Addition of 2 equiv K[N(SiMe$_3$)$_2$] (24.0 mg, 0.120 mmol) caused a clear color change to dark brown. After stirring for 3 hours, the solution was filtered through silica and evaporated. Then, it was dissolved with methanol and slow diethyl ether diffusion over the resulting solution afforded, in a few days, dark brown crystals. ESI-MS (m/z): 319.0 [Co^{III}+L]$^+$ 337.0 [Co^{III}+L+H$_2$O]$^+$, 419.0 [**2**+H]$^+$. Anal. Calcd for $C_{18}H_{23}CoN_4O_4 \cdot 1H_2O$: C, 49.55; N, 12.84; H, 5.77 %. Found: C, 49.28; N, 12.81; H, 5.38 %. ^{1}H-NMR (CD$_3$CN, 400 MHz, 298K) δ, ppm: 8.1 (t, J = 7.7 Hz, 1H, Ar**H$_a$**), 7.79 (d, J = 7.7 Hz, 2H, Ar**H$_b$**), 4.14-4.05 (m, 1H, **H$_c$**), 4.05-3.95(m, 1H, **H$_d$**), 3.60-3.49 (m, 1H, **H$_e$**), 3.31-3.20 (m, 1H, **H$_f$**), 3.19-3.08 (m, 1H, **H$_g$**), 2.81-2.70 (m, 1H, **H$_h$**), 2.25(s, 3H, L-C**H$_3$**), 1.92-1.85 (m, 1H, **H$_i$**), 1.79-1.70 (m, 1H, **H$_j$**), 1.70-1.59 (m, 2H, **Hk/l**), 1.50 (s, 3H, acac-C**H$_{3m}$**), 1.22 (s, 3H, acac-C**H$_{3n}$**). ^{13}C-NMR (CD$_3$CN, 100 MHz, 298K) δ, ppm: 206.65, 140.14, 123.34, 123.05, 99.11, 65.23, 59.98, 46.11, 44.50, 40.06, 29.90, 26.91, 25.34.

2. Characterization of 1

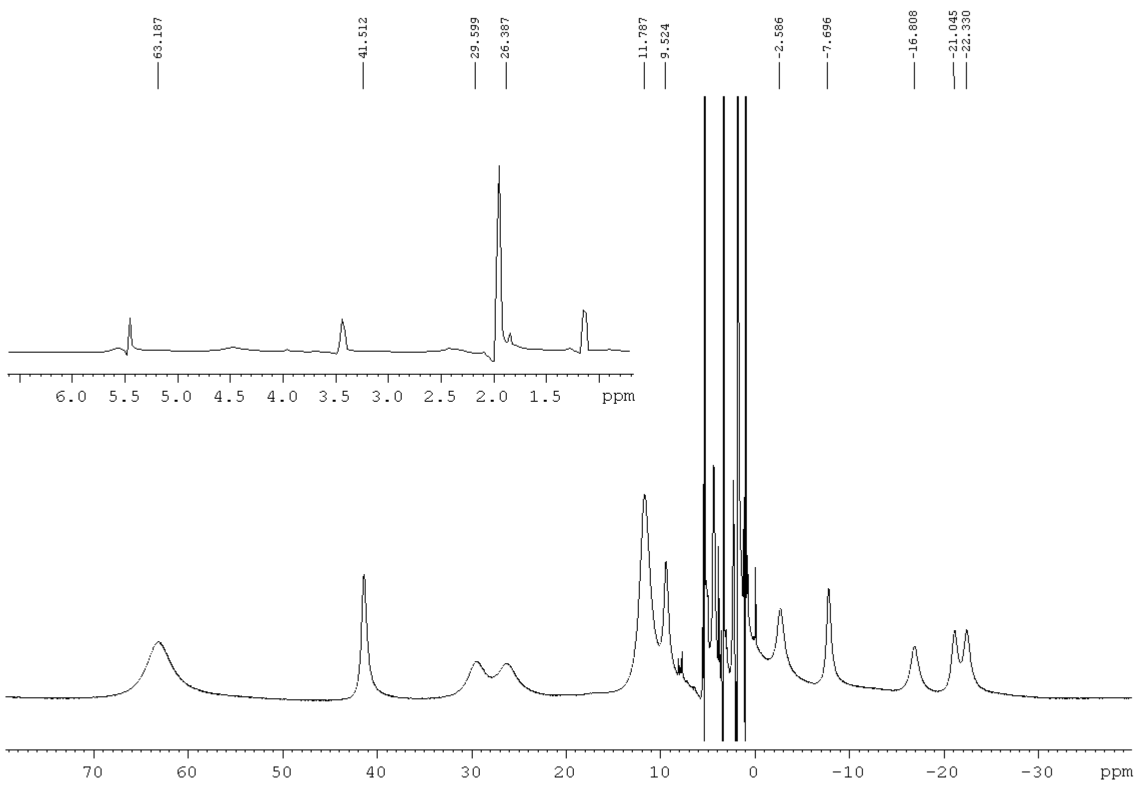

Figure S1. ^{1}H-NMR spectrum of **1** in CD_3CN at 298K (400 MHz).

Table S1. Chemical shift, relaxation time and integration of the ^{1}H-NMR spectrum of **1** in CD_3CN at 298K (400 MHz).

Chemical shift (ppm)	Relaxation time (ms)	Integration (H)
64.47	1.8	2
41.66	16	2
29.87	0.6	1
26.74	0.7	1
11.83	0.8	3
9.54	3.3	1
-2.63	2.1	2
-7.75	2.1	1
-16.92	1.9	1
-21.16	6.1	1
-22.47	5.7	1

Table S2. Crystal Data for [Co^{II}(L)]·NaBF$_4$ (**1**·NaBF$_4$).

Empirical formula	$C_{13} H_{16} B Co F_4 N_4 Na O_2$
Formula weight	429.03
Temperature	143(2) K
Wavelength	0.71073 Å
Crystal system, space group	Monoclinic, P 21
Unit cell dimensions	a = 9.991(3) Å
	α = 90 °
	b = 6.986(2) Å
	β = 112.856(5) °
	c = 12.879(4) Å
	γ = 90 °
Volume	828.4(4) A^3
Z, Calculated density	2, 1.720 Mg/m^3
Absorption coefficient	1.121 mm^{-1}
F(000)	434
Crystal size	0.30 x 0.12 x 0.08 mm
Theta range for data collection	2.211 to 24.991 °
Limiting indices	$-10 \leq h \leq 11$
	$-8 \leq k \leq 8$
	$-14 \leq l \leq 15$
Reflections collected / unique	3905 / 2514 [R(int) = 0.0401]
Completeness to theta = 28.21	96.3 %
Absorption correction	Empirical
Max. and min. transmission	1.0 and 0.417707
Refinement method	Full-matrix least-squares on F^2
Data / restraints / parameters	2514 / 145 / 271
Goodness-of-fit on F^2	1.264
Final R indices [I>2sigma(I)]	R1 = 0.0989
	wR2 = 0.2662
R indices (all data)	R1 = 0.1192
	wR2 = 0.3121
Largest diff. peak and hole	1.828 and -1.722 e.A^{-3}

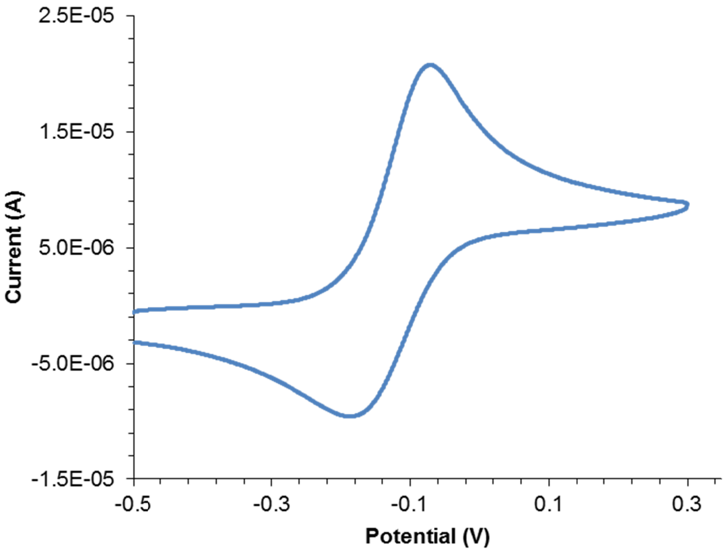

Figure S2. Cyclic voltammetry of **1** in anhydrous CH_3CN at 298 K under N_2 vs Ag/Ag$^+$.

3. Characterization of 2

Table S3. Crystal Data for [Co^{III}(L)(acac)]·H_2O (**2**·H_2O).

Empirical formula	$C_{18} H_{25} Co N_4 O_5$
Formula weight	436.34
Temperature	100(2) K
Wavelength	0.71073 Å
Crystal system, space group	Triclinic, P -1
Unit cell dimensions	a = 8.0011(15) Å
	α = 92.10(3) °
	b = 9.657(19) Å
	β = 102.94(3) °
	c = 12.97(2) Å
	γ = 105.15(3) °
Volume	938(3) A^3
Z, Calculated density	2, 1.545 Mg/m^3
Absorption coefficient	0.954 mm^{-1}
F(000)	456
Crystal size	0.08 x 0.15 x 0.20 mm
Theta range for data collection	1.6 to 28.4 °
Limiting indices	$-9 \leq h \leq 10$
	$-11 \leq k \leq 12$
	$-16 \leq l \leq 15$
Reflections collected / unique	5488 / 4040 [R(int) = 0.067]
Completeness to theta = 28.39	97.6
Absorption correction	Empirical
Max. and min. transmission	1.0 and 0.298558
Refinement method	Full-matrix least-squares on F^2
Data / restraints / parameters	4040/ 3 / 305
Goodness-of-fit on F^2	1.019
Final R indices [I>2sigma(I)]	R1 = 0.0730
	wR2 = 0.1763
R indices (all data)	R1 = 0.1047
	wR2 = 0.1980
Largest diff. peak and hole	1.339 and -0.811 e.A^{-3}

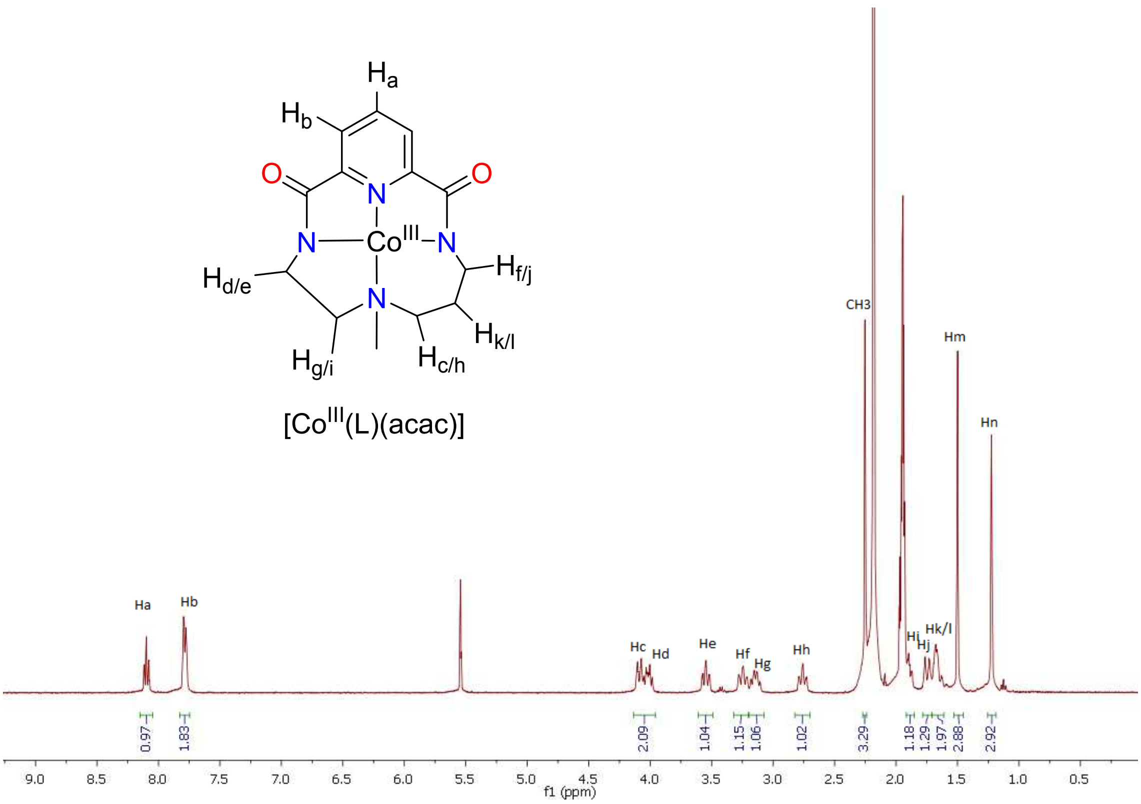

Figure S3. ^{1}H-NMR spectrum of **2** in CD_3CN at 298K (400 MHz).

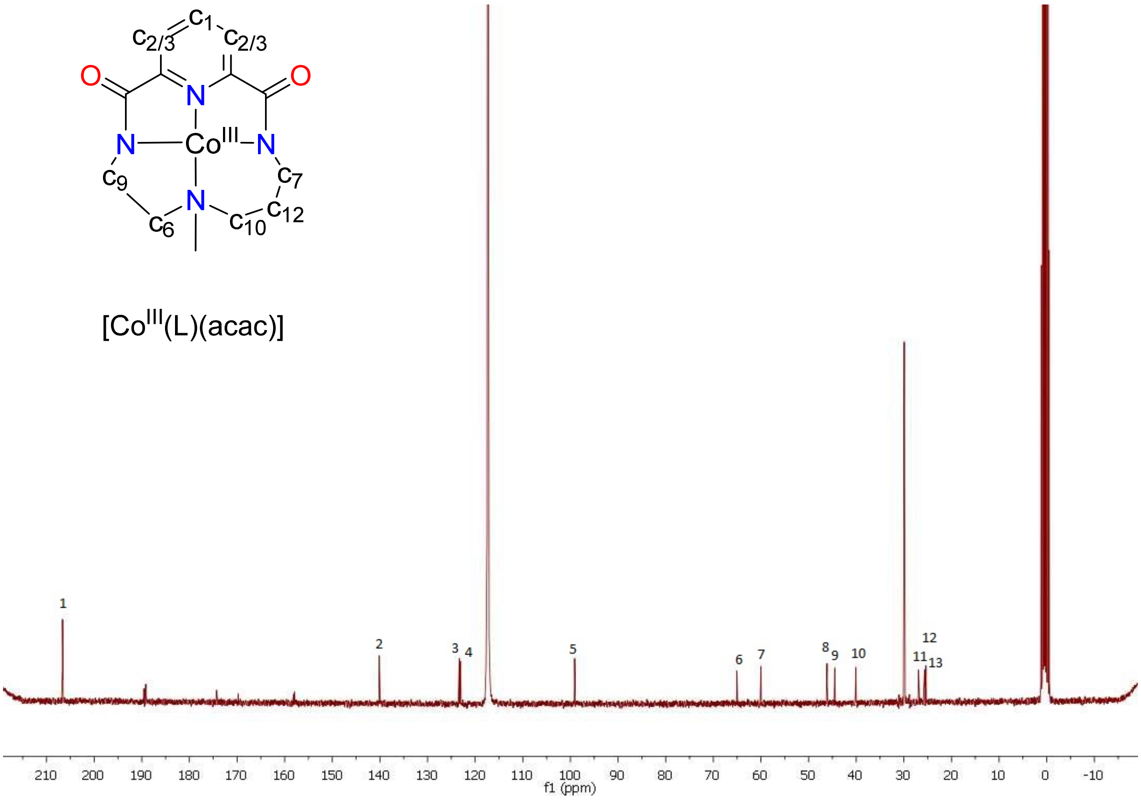

Figure S4. ^{13}C-NMR spectrum of **2** in CD_3CN at 298K (100 MHz).

4. Reaction of 1 with N_2O

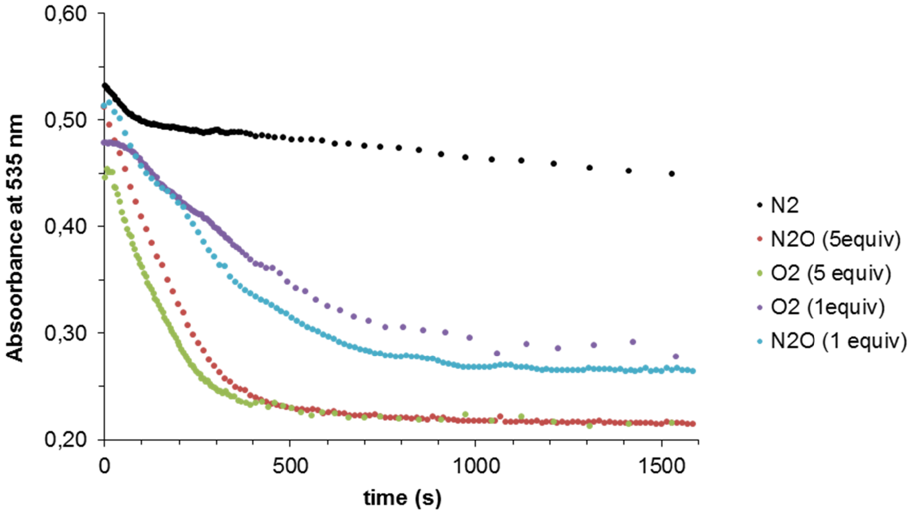

Figure S5. Kinetics traces at 535 nm of the reaction of **1** (0.5 mM) with different amounts of oxidant (N_2O or O_2) in anhydrous CH_3CN at 273 K together with a blank experiment with N_2.

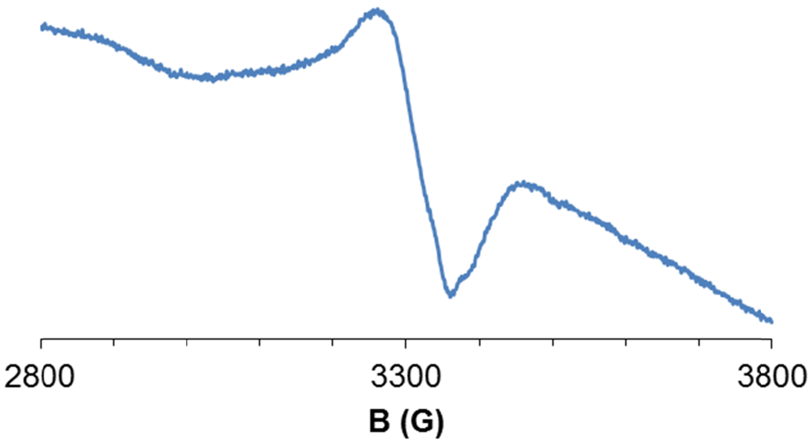

Figure S6. EPR spectrum of the reaction mixture obtained after decay of compound **1** (2 mM) upon reaction with excess N_2O in CH_3CN at 273K.

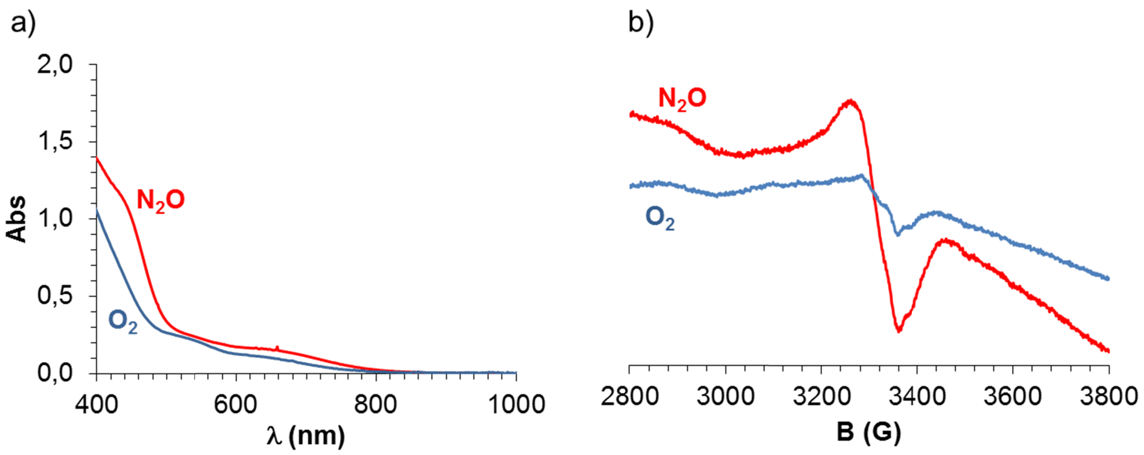

Figure S7. a) UV-vis spectra of the reaction mixture obtained after decay of compound **1** (0.5 mM) upon reaction with excess N_2O or O_2 in CH_3CN at 273 K. b) EPR spectra of the reaction mixture obtained after decay of compound **1** (2 mM) upon reaction with excess N_2O or O_2 in CH_3CN at 273 K.

Kinetic analysis of the reaction of 1 with N_2O. In a typical experiment, 2.5 mL of a 0.5 mM solution of **1** in anhydrous CH_3CN were placed in a UV-Vis cuvette (1.25 µmol of **1**). The quartz cell was capped with a septum and taken out of the glovebox, placed in the Unisoku cryostat of the UV-Vis spectrophotometer and cooled down at 273 K. After reaching thermal equilibrium a UV-Vis spectrum of the starting complex was recorded. Then, a known amount of N_2O was injected into the cell using a syringe through the septum and the process was monitored by UV-Vis. The decay of the characteristic absorption band at λ_{max} = 535 nm associated to **1** occurred in a few minutes. The reaction order with respect to **1** and N_2O was determined as follows:

a) Reaction order with respect to N_2O: under conditions of excess N_2O (5 - 100 equiv with respect to **1**) reactions showed pseudo-first-order behaviour so that the observed reaction rates (k_{obs}) were linearly dependent on the amount of N_2O (Figure 3a).

b) Reaction order with respect to **1**: the initial rates method was applied to determine the reaction order with respect to **1** by performing a series of experiments at different initial concentrations of **1** (0.1-0.8 mM) using a fixed amount of N_2O (0.13 mmol) (Figure S8).

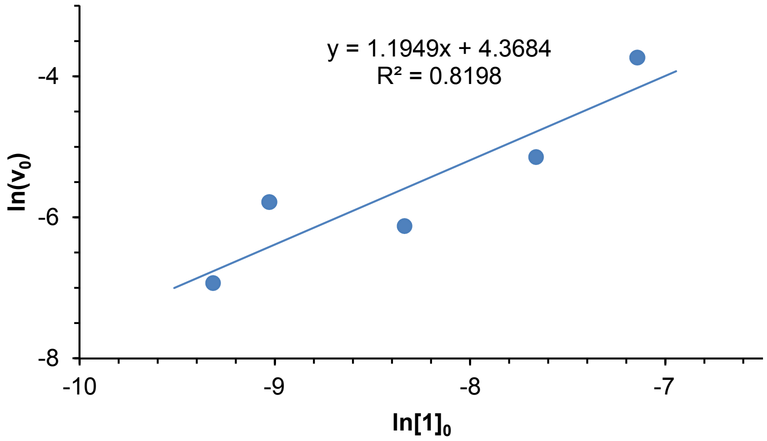

Figure S8. Plot of ln(initial rates) in front of ln[**1**]$_0$ corresponding to the reaction of **1** with N_2O (0.13 mmol N_2O) in CH_3CN at 273 K ([**1**]$_0$ = initial concentration of **1**).

Quantification of N_2 released during the reaction of 1 with N_2O. 10 mg of compound **1** (20 μmol) were dissolved in 5 mL anhydrous acetone under Ar in an encapsulated glass vial of 11 mL (capped with a septum). The vial was placed in an ice bath and under vigorous stirring excess N_2O (750 μL, 34 μmol) was injected through the septum. After 30 min, a 50 μL aliquot was extracted from the headspace and analyzed by GC-TCD. The amount of liberated N_2 was calculated by interpolation in a calibration curve (Figure S9. Standard samples were prepared as follows: 5 mL anhydrous acetone were placed in an encapsulated glass vial of 11 mL (capped with a septum) under Ar. This vial was placed in an ice bath and under vigorous stirring, 750 μL N_2O were injected through the septum. Afterwards, a known amount of N_2 (100 – 1250 μL, 4 – 56 μmol) was also introduced into the vial. After 30 min, 50 μL aliquots were extracted from the headspace of each standard sample and analyzed by GC-TCD. See the Instrumentation section above for a description of the GC-TCD columns.

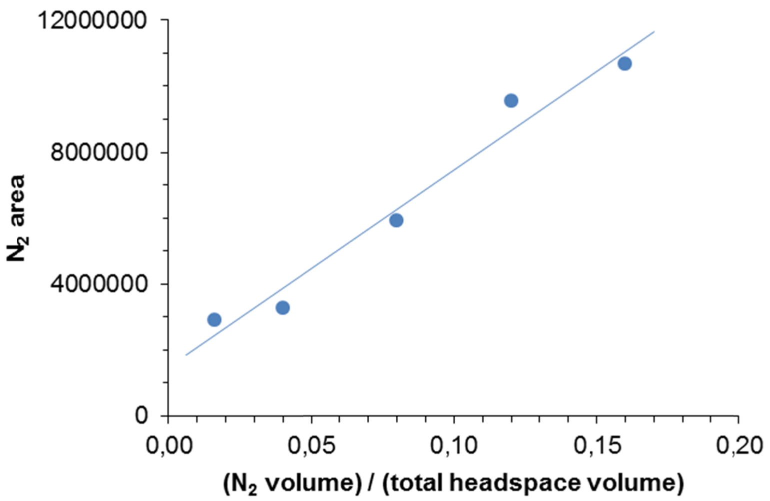

Figure S9. Calibration curve for the determination of N_2 released in the reaction of **1** with N_2O.

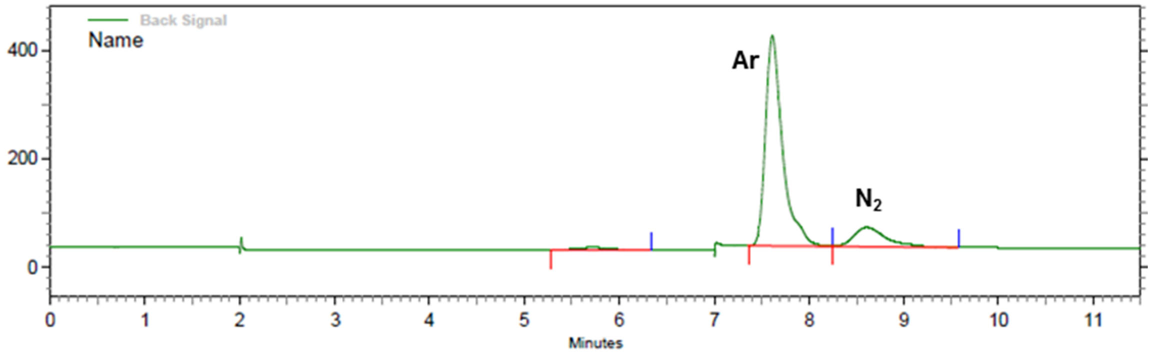

Figure S10. Gas chromatogram (GC-TCD) for the quantification of the N_2 released in the reaction of **1** with N_2O.

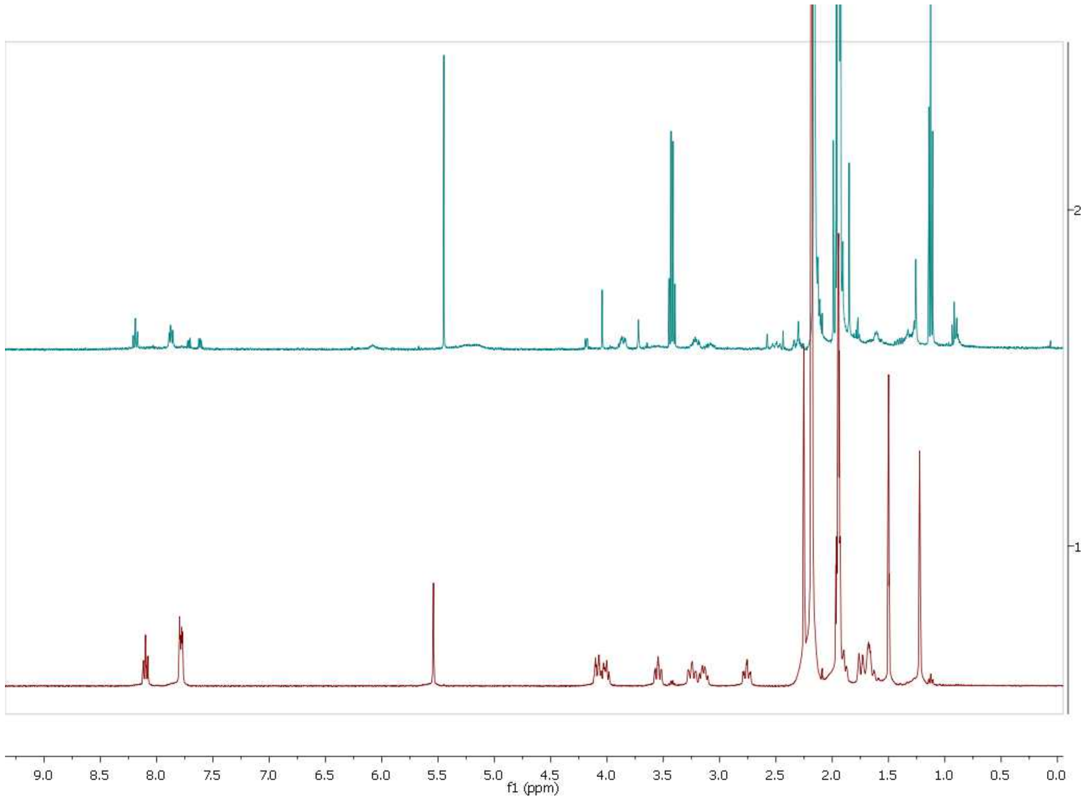

Figure S11. Top: ^{1}H-NMR spectrum of decomposed species after reaction of **1** with N_2O in CD_3CN at 298 K. Bottom: ^{1}H-NMR spectrum of **2** in CD_3CN at 298 K.

Analysis of the reaction of 1 with N_2O with cyclohexanecarboxaldehyde. In the glove box, a solution of cyclohexanecarboxaldehyde (0.2 mL, 50 equiv) in anhydrous CH_3CN was added to a stirred solution of **1** (1 equiv) in anhydrous CH_3CN (2.5 mL). Afterwards, nitrous oxide was injected into the reaction vessel using a balloon. The resulting mixture was stirred at room temperature for a given time. Biphenyl was added as internal standard and the cobalt complex was removed by passing the solution through a short path of silica. The products were then eluted with ethyl acetate and analyzed by GC-FID. The organic products were identified by comparison with authentic compounds. All reactions were run in triplicate and the results are the average of the three replicates.

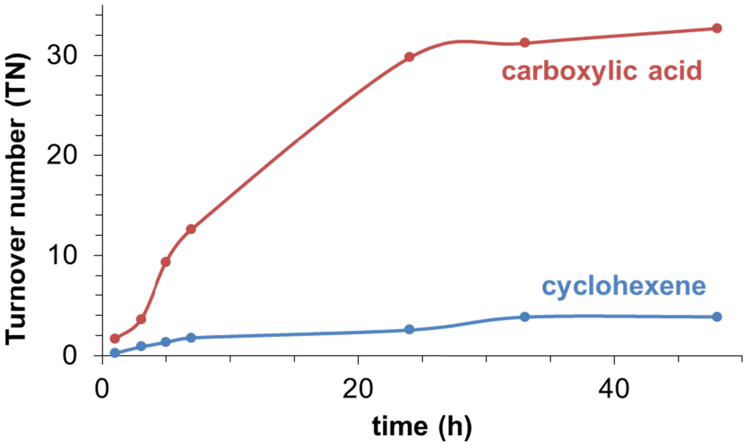

Figure S12. Evolution of cyclohexanecarboxylic acid and cyclohexene production in the reaction of **1** with cyclohexanecarboxaldehyde in the presence of N_2O in CH_3CN. A blank experiment without **1** afforded only 0.5 TN cyclohexene and 4.8 TN cyclohexanecarboxylic acid after 48 hours of reaction.

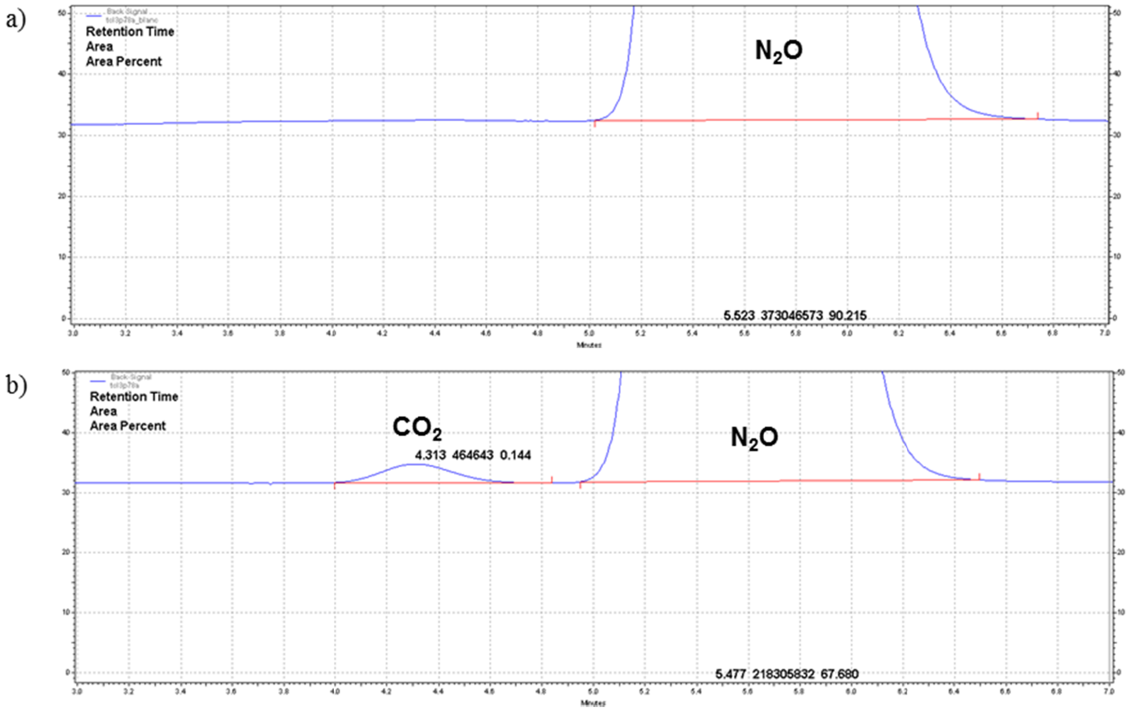

Figure S13. Gas chromatogram (GC-TCD) for the qualitative evaluation of CO_2 release in the reaction of **1** with N_2O in CH_3CN at 273 K (b) together with a blank experiment in the absence of **1** (a).